Available online at www.sciencedirect.com
ScienceDirect
Journal of the European Ceramic Society 27 (2007) 2455–2461
www.elsevier.com/locate/jeurceramsoc

Production and properties of substituted $LaFeO_3$-perovskite tubular membranes for partial oxidation of methane to syngas

Defne Bayraktar [a,*], Frank Clemens [a], Stefan Diethelm [b], Thomas Graule [a], Jan Van herle [c], Peter Holtappels [a]

[a] *Empa Swiss Federal Laboratories for Materials Testing and Research, Laboratory for High Performance Ceramics, Überlandstr. 129, CH-8600 Dübendorf, Switzerland*
[b] *HT Ceramix SA, Av. Des Sports 26, CH-1400 Yverdon-les-Bains, Switzerland*
[c] *Ecole Polytechnique Fédérale de Lausanne (EPFL), Laboratory for Industrial Energy Systems (LENI), STI, CH-1015 Lausanne, Switzerland*

Received 10 August 2006; received in revised form 4 October 2006; accepted 16 October 2006
Available online 5 December 2006

Abstract

Tubular membranes of $La_{0.6}Ca_{0.4}Fe_{0.75}Co_{0.25}O_{3-\delta}$ and $La_{0.5}Sr_{0.5}Fe_{1-y}Ti_yO_{3-\delta}$ ($y = 0$, 0.2) for the application of partial oxidation of methane to syngas were produced by thermoplastic extrusion and investigated by oxygen permeation measurements. The optimum ceramic content in the feedstock for extrusion was found to be 51 vol% as a result of rheology measurements. Tubes with an outer diameter of 4.8–5.5 mm and thickness of 0.25–0.47 mm were produced with densities higher than 95% of the theoretical density. The oxygen permeation flux of the tubular membranes was measured with air on one side and Ar or Ar + CH_4 mixture on the other side. The oxygen permeation rate decreased with Ti-substitution while it was considerably increased by introduction of 5% methane into the system. The normalized oxygen fluxes in air/Ar gradient at 900 °C were measured to be 0.06, 0.051, and 0.012 μmol cm^{-2} s^{-1} for LCFC, LSF, and LSFT2, respectively, and 0.18 μmol cm^{-2} s^{-1} for LSFT2 with 5% methane.

Keywords: Extrusion; Perovskites; Membranes; Oxygen permeation flux; $LaFeO_3$

1. Introduction

Mixed ionic electronic conducting perovskites or related materials receive considerable attention for the application of oxygen separation membranes for air separation (e.g. medical O_2) and partial oxidation (e.g. syngas production from methane).[1–4] These membranes have potential to be integrated in industrial processes that require pure oxygen and are of growing interest considering economical and environmental aspects.[5] Ceramic membranes conduct oxygen ions at elevated temperatures via oxygen vacancies. A lot of effort is focused especially on perovskite materials because of their ability to tolerate high amount of non-stoichiometry, which allows them to show high oxygen ionic conduction. However, the challenge in real applications of these materials is the lack of chemical and mechanical stability.[6] Especially in syngas production, the large pO_2-gradient causes serious chemical expansion in addition to chemical instability. Therefore, the candidate materials should sustain stability over a wide range of pO_2. Among several compositions, ferrites[7–12] and cobaltites[13–15] have been studied most extensively, while (La,Sr)FeO_3-based materials have received special interest because they show better stability compared to the Co-containing compositions.[16]

The stabilities of the materials are commonly improved by B-site doping with a more stable cation such as Cr, Al, Ga, etc.[12,17–19], however, most of the additions are reported to cause a decrease in ionic conductivity with exception of Ga[20] in oxidizing conditions. In the case of chromites, Ti was mentioned as the substitution element on the B-site that leads to a particularly low vacancy formation upon reduction compared to several others.[17]

In the presented work, $LaFeO_3$ was chosen as the base material with Ca or Sr substitution on the A-site and Co or Ti on the B-site. $La_{0.6}Ca_{0.4}Fe_{0.75}Co_{0.25}O_{3-\delta}$, $La_{0.5}Sr_{0.5}FeO_{3-\delta}$, and $La_{0.5}Sr_{0.5}Fe_{0.8}Ti_{0.2}O_{3-\delta}$ tubes were produced by thermoplastic extrusion and their oxygen permeation behavior was examined

* Corresponding author.
E-mail address: defne.bayraktar@empa.ch (D. Bayraktar).

0955-2219/$ – see front matter © 2006 Elsevier Ltd. All rights reserved.
doi:10.1016/j.jeurceramsoc.2006.10.004

under air/Ar gradient. (La,Ca)(Fe,Co)$O_{3-\delta}$ materials were reported to become instable with increasing amount of Co on the B-site.[13] Therefore, 25% Co on the B-site was used for B-site substitution. $La_{0.5}Sr_{0.5}FeO_{3-\delta}$ was reported to possess the highest ionic conductivity in this series of materials with Sr-substitution on the A-site.[7] In addition, 20% Ti was used as a dopant on the B-site as a stabilizing cation. The previous work conducted on similar materials showed that the Ti-doping on the B-site decreases oxygen permeability, ionic conductivity, and as well the thermal expansion.[12]

Tubes rather than plates are preferable for oxygen separation membranes considering the mechanical stability, effectiveness, and the ease of application, e.g. for sealing purposes. Thermoplastic extrusion has been used by several groups to produce perovskite tubes of different compositions.[21–23] Very good mechanical stability of the green body is a big advantage considering the handling of the samples and this provides the possibility to produce tubes with thin walls (<200 μm).

2. Experimental procedure

2.1. Sample preparation

$La_{0.6}Ca_{0.4}Fe_{0.75}Co_{0.25}O_{3-\delta}$ and $La_{0.5}Sr_{0.5}Fe_{1-x}Ti_xO_{3-\delta}$ ($x = 0$, 0.2) powders (abbreviated as LCFC, LSF and LSFT2, respectively) were prepared by solid state reaction of the reagents $La(OH)_3$, $SrCO_3$, $CaCO_3$, Fe_2O_3, CoO, and TiO_2. Homogeneous mixtures were obtained by ball-milling the powders with an organic processing aid (Dolapix CE 64). Powders were calcined at 1250 °C for 4 h following the spray-drying process. The phase-purity of the calcined powders was examined by XRD (X'pert PRO PW3040, PANalytic). Afterwards, the powders were ball-milled in order to obtain a particle size in the range of 1–2 μm and spray-dried again. The particle size distribution of the powders was measured with a laser diffraction analyzer (LS230, Beckman-Coulter, USA). The specific surface area (SSA) of the powders was determined from a five point N_2 adsorption isotherm obtained from BET (Brunauer–Emmett–Teller) measurements using a Beckman-Coulter SA3100 (Beckman-Coulter, USA). The actual compositions of the materials were checked by XRF.

Tubes of compositions LSF and LSFT2 with outer diameter of 4.8–6 mm and wall thickness of 0.25–1.1 mm after sintering were produced by thermoplastic extrusion. Thermoplastic feedstocks were prepared with filling levels between 44 and 54.5 vol%. Licamont wax (EK 583, Clariant GmbH, Germany) and a polyethylene (PE) binder (1700MN 18C Lacqtene PEBD, elf atochem S.A., Switzerland) were mixed with ceramic powder in a high-shear mixer (Rheomix 3000 Torque Rheometer, Thermo Electron Corporation, Germany) in the temperature range of 110–170 °C. In order to study the optimum ceramic content of the feedstock, several batches with different filling levels (44, 46, 48, 51, 53, and 54.5 vol%) were produced from LCFC material. A kneader with a volume of 69 cm^3 was used for the preparation of different ceramic contents, while a bigger kneader with a volume of 310 cm^3 was used for the feedstock, which was used for the extrusion of tubes. In order to reach maximum efficiency, the kneading volume was filled to 70%.

The rheological behavior of the feedstocks was analyzed by a twin-bore capillary rheometer (RH7-2, Rosand Precision Limited, Germany). A single screw extruder (Rheomix 202, Thermo Electron Corporation, Germany) was used for extrusion of the tubes. The tubes were sintered at 1300, 1430, and 1530 °C for 4 h for LCFC, LSF, and LSFT2, respectively. A slow heating curve was applied before sintering for binder removal. The microstructures of the sintered samples were investigated by SEM (Vega© Tescan).

2.2. Oxygen permeation measurements

Characterization of the oxygen transport properties was made on a system where a tube was fixed at the ends to alumina tubes with gold-paste. Then they were introduced in a quartz-tube (with 10 mm internal diameter). The space between the measured mixed-conducting tube and the quartz-tube was filled with MgO granulates (∼1 mm in diameter) coated with the catalyst. Ar or methane–Ar mixture was fed to this catalytic side and air to the inner side. Gas flow rates of 100 ml/min were used for both sides. The composition of the outlet gas from the catalytic side was analyzed using a gas chromatograph (Varian). A more detailed explanation of this system is given elsewhere.[21] The permeation measurements were conducted during cooling from 1000 to 750 °C at each 50 K after a certain dwell time for equilibration.

3. Results and discussion

3.1. Powder fabrication

The powders produced revealed no considerable second-phase formation according to X-ray diffraction measurements. The XRD patterns of all compositions are shown in Fig. 1. LSF was found to have a hexagonal structure with unit cell parameters of $a = b = 5.5091$, and $c = 6.7029$ Å ($V = 176.18$ Å^3). In the JCPDS XRD database the structure is reported as rhombohedral (R-3c) with $a = 5.5111$ and $c = 13.4158$ Å ($V = 352.87$ Å^3) (01-082-1962). In literature the structure is

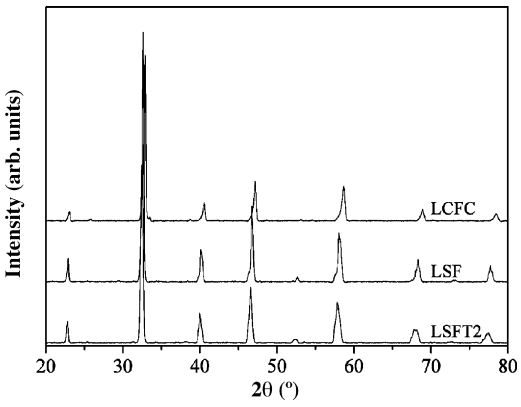

Fig. 1. XRD patterns of LCFC, LSF, and LSFT2.

Table 1
Abbreviations, mean particle sizes (from laser diffraction and SSA), and SSAs of the powders

Composition	Abbreviation	d_{50} (μm)	SSA (m^2/g)	d_{50} (SSA) (μm)
$La_{0.6}Ca_{0.4}Fe_{0.75}Co_{0.25}O_{3-\delta}$	LCFC	2.0	1.60	0.63
$La_{0.5}Sr_{0.5}FeO_{3-\delta}$	LSF	1.3	1.89	0.51
$La_{0.5}Sr_{0.5}Fe_{0.8}Ti_{0.2}O_{3-\delta}$	LSFT2	2.1	1.32	0.75

reported as rhombohedral with the same space group with $a = 0.54927$ nm, and $\alpha = 60.27°$.[12] It can be concluded that the structures are in agreement considering that the hexagonal structure can be defined by rhombohedral lattice by adopting the axes and that the unit cell volume reported in the database is double of what is found in this study. XRF analyses of the powders showed that the compositions were slightly La-deficient.

The average particle size distribution by laser diffraction analyzer showed a Gaussian distribution. The average particle size (d_{50}) and the specific surface areas (SSA) measured by BET are shown in Table 1. The SEM micrograph of spray-dried $La_{0.5}Sr_{0.5}FeO_{3-\delta}$ particle is shown in Fig. 2. The spray-drying results in spherical particles as big as 50 μm composed of loosely bound crystallites. This provides easier flow of particles, which is advantageous for processing. It can be seen in the micrograph of the spray-dried powder that in average the particle size of crystallites is less than 1 μm, although there are some bigger ones. This suggests that the presence of aggregates results in a higher value of average particle size in laser diffraction analysis. This is supported by the average particle sizes calculated from SSA (Table 1). Although the trend is the same among the powders, the values are less than half of the sizes measured by laser diffraction. Note that, it is assumed that the particles are spherical and uniform in d_{50} (SSA) calculations.

3.2. Tube fabrication

In the preparation of feedstock for extrusion of tubes, it is important to use the right amount of ceramic powder. It has to be high enough to conserve the shape of the extruded tube as well as to obtain a good density after sintering. However, the ceramic powder content should be low enough to prevent abrasion during high-shear mixing and forming process by extrusion. Therefore, the viscosities of the feedstocks with different solid contents were measured as a function of shear rate, which is shown in Fig. 3. Following shear thinning behavior, the viscosity decreased with increasing shear rate for all feedstocks. The viscosity was found to be similar for solid contents of 44–48 vol% while it was considerable higher for 51 vol%. It is assumed that the wax dominate the viscosity behavior of the feedstock. Note that, the weight ratio of binder/wax (PE/Licomont) in the system was increased slightly (from 0.12 to 0.16) for the feedstocks with solid content more than 51% because of the mechanical instability of the extruded tubes. For 53 and 54.5 vol% feedstocks, the slopes of the viscosity curves increased. Because of the molecular structure, PE shows a stronger shear thinning effect, therefore, the viscosities at higher shear rates for different PE amounts are similar.

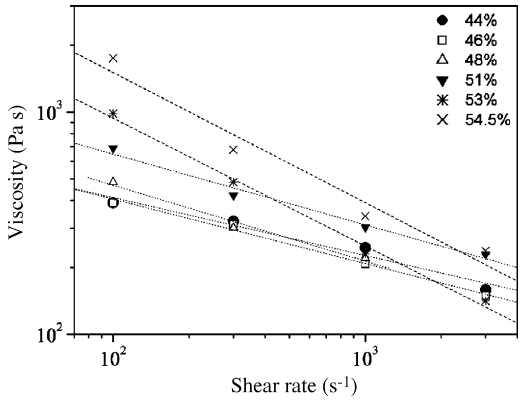

Fig. 3. Viscosity of the LCFC feedstock with different solid loading as a function of shear rate.

The torque values reached after the homogenization of the kneaded materials are shown in Fig. 4 as a function of solid content. The so-called equilibrium torque is increasing with increasing solid content up to 51 vol% and remains almost constant, because of the different binder system. However, although the torque does not increase, it starts to fluctuate more after 51 vol% ceramic as can be seen from the error bars. This is

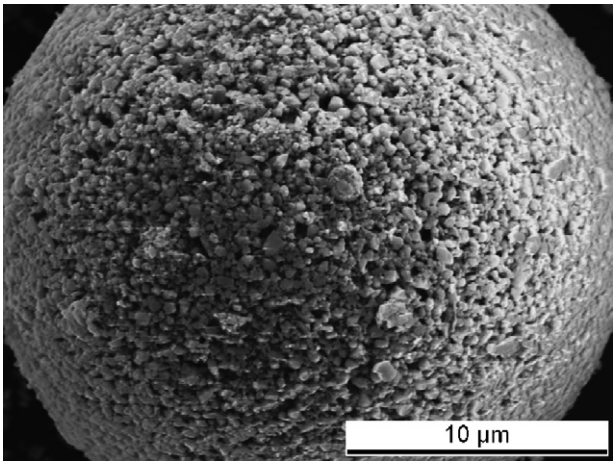

Fig. 2. SEM-micrograph of spray-dried LSF powder.

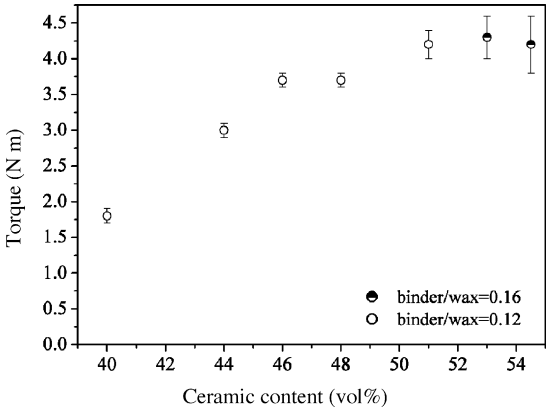

Fig. 4. Equilibrium torque of kneading as a function of ceramic content for LCFC.

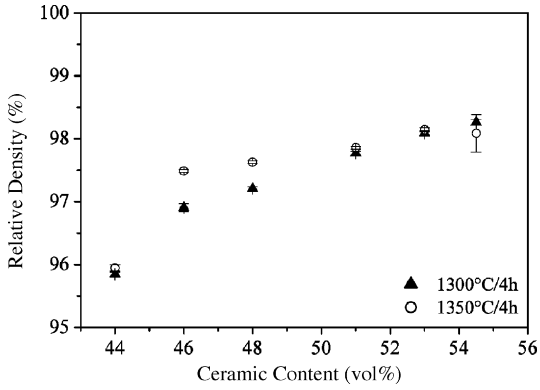

Fig. 5. Relative densities of the LCFC samples sintered at 1300 and 1350 °C as a function of ceramic content.

a sign of inefficient mixing, which means considerably longer kneading time is necessary to get a homogenous feedstock. As a result, 51 vol% solid loading was found to be optimal for thermoplastic extrusion of perovskite materials given that the powder characteristics are similar.

The densities of the sintered (at 1300 and 1350 °C for 4 h) samples are shown in Fig. 5. The relative density increases with increasing solid content and sintering temperature, reaching 98% for the feedstock with 51 vol% ceramic. No significant influence of the higher sintering temperature was observed for the feedstocks with ceramic content more than 51 vol%.

Although slightly improved by increasing the PE amount, the extruded tubes of LCFC were observed to be very brittle compared to extruded tubes of some other materials (e.g. ZrO_2), which is disadvantageous for handling. Therefore, the ratio of PE/Licomont in the binder system was increased to 0.5 for the thermoplastic extrusion of LSF and LSFT2 materials. The equilibrium torque was lower in this case (12 and 14 Nm for LSF and LSFT2, respectively), compared to LCFC (17 Nm). This observation supports the previous result that increasing the amount of PE decreases the torque and therefore the abrasion during processing. This can be explained by lower interaction between the particles because of the higher molecular weight of the PE compared to the wax. In addition, no strong fluctuation in the torque was observed for these feedstocks indicating that for LSF and LSFT2 the PE/Licamont ratio used was suitable for an efficient high-shear mixing.

Extrusion of straight tubes was found to be strongly dependent on the environment conditions since bending was observed in different directions. Straight tubes could be obtained by preventing any kind of air-flow until the tubes cooled down to room temperature. In recent investigations in our lab, this sort of bending by inhomogeneous cooling was attributed to the partial crystallization of PE during cooling.

The relative densities of the sintered samples are shown in Table 2 together with the dimensions of the tubes used for permeation measurements. Typical microstructures of fractured surfaces of sintered tubes are shown in Fig. 6. The samples show

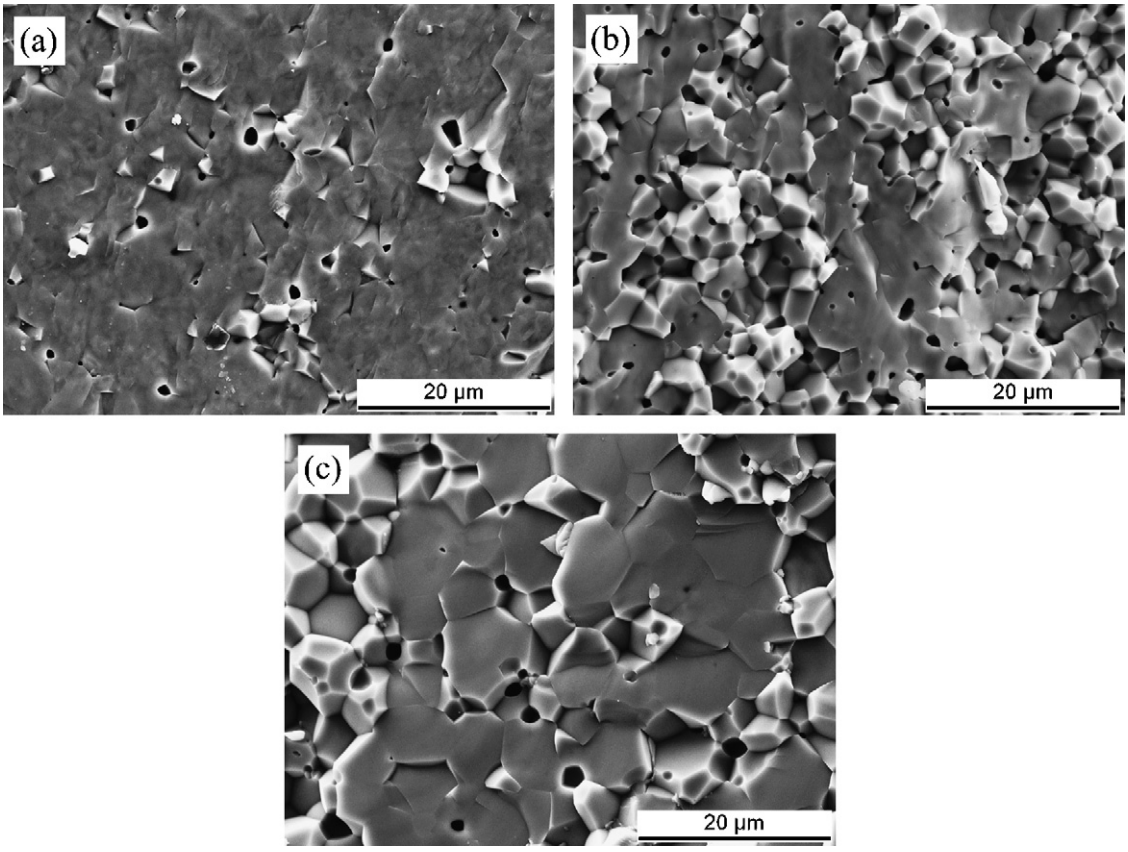

Fig. 6. Fracture surfaces of sintered (a) LCFC, (b) LSF, and (c) LSFT2 tubes.

Table 2
Physical properties of the tubes measured for oxygen permeation flux

Sample	Relative density (%)	Outer diameter (mm)	Wall thickness (mm)
LCFC	97.1 ± 0.1	5.50 ± 0.02	0.25 ± 0.01
LSF	95.8 ± 0.7	5.00 ± 0.02	0.47 ± 0.01
LSFT2	95.1 ± 0.2	4.80 ± 0.03	0.36 ± 0.02

intragranular fracture, which is more pronounced in the LCFC sample of higher density.

3.3. Oxygen permeation

Arrhenius plots of oxygen permeation flux for a fixed air/Ar gradient are shown in Fig. 7. The data was normalized by multiplying the flux with the membrane thickness to be able to make a comparison between the compositions assuming that the flux is governed by bulk transport instead of surface exchange. Note that it was mentioned by Diethelm et al.[21] that the oxygen transport for LCFC was governed by bulk transport below 900 °C in air/Ar gradient since the normalized flux of membranes with thicknesses of 0.25 and 1.26 mm were very similar. In LSF planar membranes, the oxygen flux was found to be surface limited at 850 °C and below the thickness of 0.49 mm in air.[24]

Comparing the normalized fluxes, the LSFT2 tube exhibited lower permeation and higher activation energy compared to the LSF tube. The activation energies (E_A) calculated for LSF and LSFT2 are 76 and 150 kJ/mol, respectively. The LCFC membrane has activation energies of 93 kJ/mol above 900 °C and 151 kJ/mol below 900 °C. The actual oxygen permeation fluxes at 900 °C are 0.24, 0.11, and 0.034 μmol cm^{-2} s^{-1} for LCFC, LSF, and LSFT2, respectively. It is known that the substitution of Fe with a cation that has lower reduction stability increases the oxygen flux assuming the composition stays stable as in this case of Co-substitution.[13] Although it is not possible to make a direct comparison in this case because of the different A-site compositions, LCFC was found to have slightly higher flux (normalized) at temperatures higher than 900 °C. On the other hand, as a more stable cation, Ti-substitution is expected to lower the

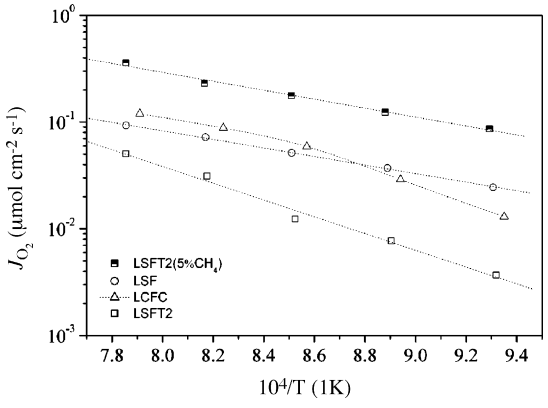

Fig. 7. Arrhenius plot of normalized oxygen permeation flux through LCFC,[21] LSF, and LSFT2 tube membranes under air/Ar gradient and LSFT2 under air/Ar + 5%CH_4 gradient.

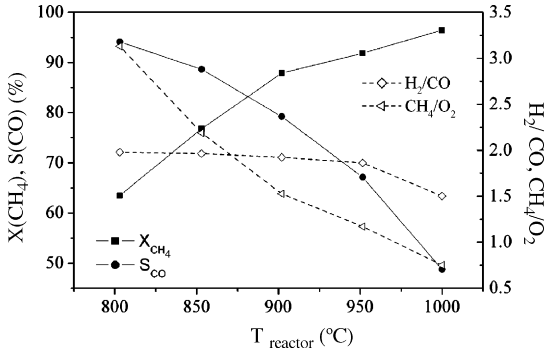

Fig. 8. Catalytic performances of a tubular LSFT2 POX reactor as a function of temperature under Ar + 5%CH_4 flow.

flux, which is reported in other studies by Tsipis et al.[12] Permeation measurements by the authors on planar membranes of the LSF and LSFT2 compositions revealed that there were discontinuities in the Arrhenius plots for both cases.[24] Below the discontinuity temperature the equilibration of the flux was found to be very slow and this was attributed to possible ordering of oxygen vacancies. This behaviour was not observed in the case of tubes.

In order to prevent an abrupt change in the material, CH_4 was introduced to the catalytic side gradually. Although it was possible to measure the oxygen flux of LCFC with pure methane as published before,[21] there were problems with LSF and LSFT2 membranes. The LSF membrane fractured with introduction of CH_4 while an LSFT2 membrane could be measured up to 5%CH_4 + Ar. The Arrhenius plot for LSFT2 measured with 5%CH_4 + Ar is shown in Fig. 7. The oxygen permeation at 900 °C was increased to 0.49 μmol cm^{-2} s^{-1}, a factor of 14 compared to argon atmosphere. However, a leakage was observed when increasing the amount of methane to 10% at 1000 °C. This indicates that the stability limit of the membrane material was exceeded. On the other hand, LCFC was reported to reach an oxygen flux of 2 μmol cm^{-2} s^{-1} at 900 °C with 100% CH_4.[21] Moreover, the reactor operated stably for 1400 h from which 600 h were under pure methane.

The performance of a LSFT2 tube under 5%CH_4 flow is shown in Fig. 8. Evaluation was done for the gas composition of the outlet gas and using conservation equations. A more detailed explanation of the procedure is given elsewhere.[21] The abbreviations have the following meanings: X_{CH_4} = methane conversion, S_{CO} = CO selectivity. The methane conversion reaches a value of 87% at 900 °C and 96.4% at 1000 °C while CO selectivity is 79% at 900 °C and lowered to 49% at 1000 °C. However, the main focus of this test was to evaluate the increase in flux by introducing methane on the permeation side. As it can be seen in Fig. 8, the methane inlet was not adjusted to the oxygen permeation flux; therefore the CH_4/O_2 varies from 0.75 to 3, which explains the changes in CO selectivity and methane conversion.

The post-mortem analysis of LCFC membrane measured as a POX-reactor were presented in an earlier publication.[21] Fig. 9 shows the SEM micrographs of the LSF and the LSFT2 tubes after the permeation tests under air/Ar and air-5%CH_4 + Ar

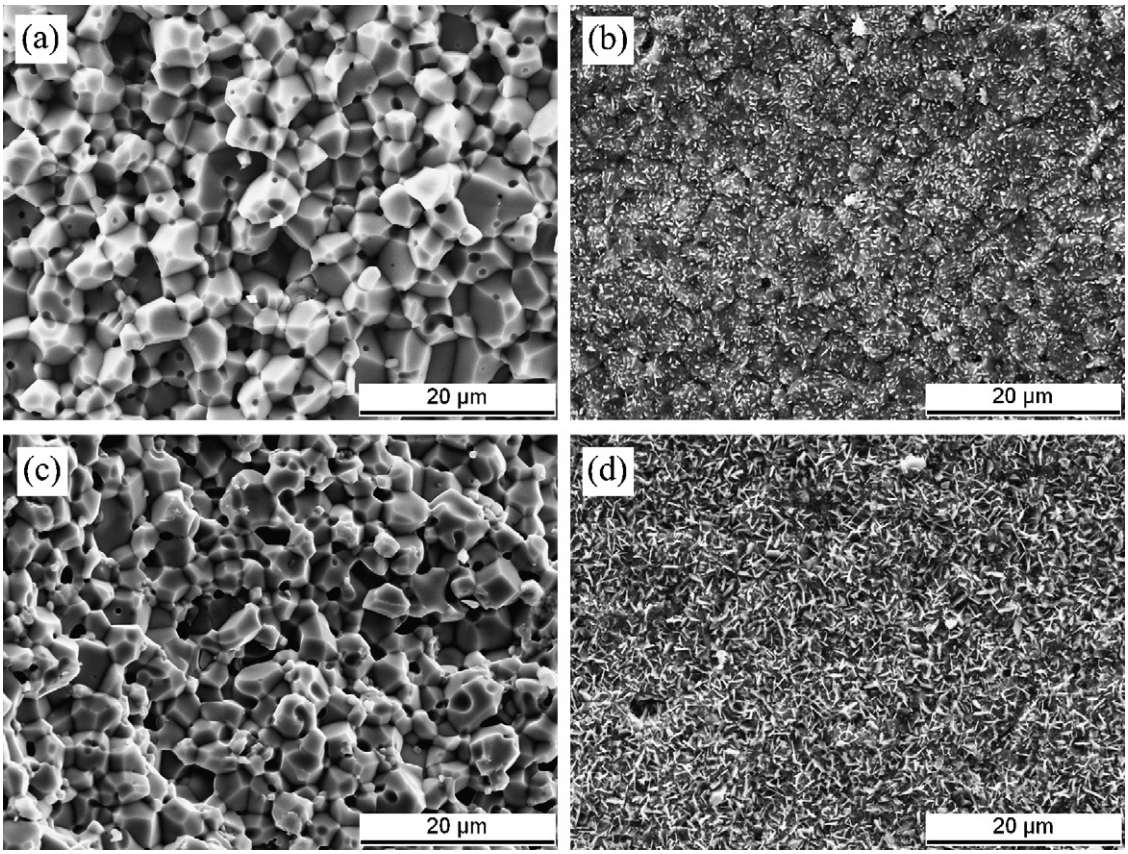

Fig. 9. SEM micrographs of (a) the fracture surface, (b) the inner surface of the LSF-tube measured under air/Ar gradient, (c) the fracture surface, and (d) the inner surface of LSFT2 tube measured under air-(5%CH_4 + Ar) gradient.

atmospheres, respectively. In the Fig. 9, (a) and (b) show the fracture and inner (air) surfaces of LSF while (c) and (d) are the fracture and inner (air) surfaces of LSFT2, respectively. According to back scattered (BSE) image there was no obvious change in the composition throughout the thickness of the membrane for both LSF and LSFT2. However, fine structures were formed on the air-exposed surface of the tubes, which were not easy to differentiate in the back scattered image. The amount of the second-phase formed is more pronounced in the case of LSFT2 covering the whole surface (Fig. 9(d)). These structures may be result of contamination from outside or beginning of phase decomposition as reported for LCFC.[21] Further investigations are necessary to conclude the preliminary results.

The fracture of the ceramics is mostly intergranular in this case after operation while it is a mixture of inter- and intragranular in the case of as-sintered tubes (Fig. 6). This suggests a structural change in the grain boundaries ending up in weaker boundaries, in good agreement with the observation that the materials were considerably more brittle after the permeation measurements. A possible explanation for this behaviour may be related to the high thermal and isothermal expansion coefficients of the LSF materials.[12,25] It is known that the isothermal expansion is a result of the gradual reduction of the B-site cation resulting in a larger cation radius.[17] The difference in the local pO_2 through the membrane may therefore cause internal stresses resulting in micro cracks and lower mechanical stability. Furthermore, the difference in the expansion behaviour of the grains and grain boundaries may become more pronounced with increased chemical expansion of the material. These could explain the difficulties faced in permeation measurements under methane atmosphere as well.

4. Conclusion

Tubular membranes of $La_{0.6}Ca_{0.4}Fe_{0.75}Co_{0.25}O_{3-\delta}$ and $La_{0.5}Sr_{0.5}Fe_{1-y}Ti_yO_{3-\delta}$ ($y = 0$, 0.2) were produced by thermoplastic extrusion. Thermoplastic feedstocks with different ceramic content were produced and their viscosities measured as a function of the shear rate. About 51 vol% ceramic content was found to be optimum for tube production. Straight tubes could be obtained with outer diameter of 4.8–5.5 mm and thickness of 0.25–0.47 mm. The sintered tubes had more than 95% of theoretical density.

The oxygen permeation flux of the tubular membranes were measured in a system where air was introduced through the inner side of the tube and Ar or Ar + CH_4 mixture was introduced in the outer catalytic side, which was covered with a oxide-based catalytic layer. The oxygen fluxes in an air/Ar gradient at 900 °C were measured to be 0.24, 0.11, and 0.034 μmol cm^{-2} s^{-1} for LCFC, LSF, and LSFT2, respectively; 0.49 μmol cm^{-2} s^{-1} for LSFT2 with 5% methane. The Ti-substitution decreased the oxygen permeation rate. On the other hand, it increased the sta-

bility of the LSF membrane allowing operation in 5% CH_4 + Ar atmosphere. The LCFC shows a superior stability at similar permeation rates allowing operation in pure CH_4 over several hundreds of hours. Therefore, LSF materials need to be optimized considering their stability and oxygen permeation flux. Although both materials show reasonable fluxes, they need to be improved further for technical applications.

Acknowledgement

This work was supported by Swiss National Science Foundation (Project 200021-100674/1). The oxide-based catalyst was produced by HTCeramix SA.

References

1. Bouwmeester, H. J. M. and Burggraaf, A. J., Dense ceramic membranes for oxygen separation. In *CRC Handbook of Solid State Electrochemistry*, ed. P. J. Gellings and H. J. M. Bouwmeester. CRC Press, Boca Raton, New York, London, Tokyo, 1997, pp. 519–542.
2. Steele, B. C. H., Dense ceramic ion conducting membranes. In *Oxygen Ion and Mixed Conductors and Their Technological Applications, Series E, Nato ASI Series*, *vol. 368*, ed. H. L. Tuller, 2000, pp. 245–323.
3. Ullmann, H. and Trofimenko, N., Composition, structure and transport properties of perovskite-type oxides. *Solid State Ionics*, 1999, **119**, 1–8.
4. Balachandran, U. and Ma, B., Mixed-conducting dense ceramic membranes for air separation and natural gas conversion. *J. Solid State Electrochem.*, 2006, **10**, 617–624.
5. Dyer, P. N., Richards, R. E., Russek, S. L. and Taylor, D. M., Ion transport membrane technology for oxygen separation and syngas production. *Solid State Ionics*, 2000, **134**, 21–33.
6. Hendriksen, P. V., Larsen, P. H., Mogensen, M., Poulsen, F. W. and Wiik, K., Prospects and problems of dense oxygen permeable membranes. *Catal. Today*, 2000, **56**, 283–295.
7. Patrakeev, M. V., Bahteeva, J. A., Mitberg, E. B., Leonidov, I. A., Kozhevnikov, V. L. and Poeppelmeier, K. R., Electron/hole and ion transport in $La_{1-x}Sr_xFeO_{3-\delta}$. *J. Solid State Chem.*, 2003, **172**, 219–231.
8. ten Elshof, J. E., Bouwmeester, H. J. M. and Verweij, H., Oxygen transport through $La_{1-x}Sr_xFe_{O3-\delta}$ membranes. I. Permeation in air/He gradients. *Solid State Ionics*, 1995, **81**, 97–109.
9. ten Elshof, J. E., Bouwmeester, H. J. M. and Verweij, H., Oxygen transport through $La_{1-x}Sr_xFeO_{3-\delta}$ membranes. II. Permeation in air/CO, CO_2 gradients. *Solid State Ionics*, 1996, **89**, 81–92.
10. Yoo, J., Park, C. Y. and Jacobson, A. J., Determination of the equilibrium oxygen non-stoichiometry and the electrical conductivity of $La_{0.5}Sr_{0.5}FeO_{3-\delta}$. *Solid State Ionics*, 2004, **175**, 55–58.
11. Mizusaki, J., Yoshihiro, M., Yamauchi, S. and Fueki, K., Nonstoichiometry and defect structure of the perovskite-type oxides $La_{1-x}Sr_xFeO_{3-\delta}$. *J. Solid State Chem.*, 1985, **58**, 257–266.
12. Tsipis, E. V., Patrakeev, M. V., Kharton, V. V., Yaremchenko, A. A., Mather, G. C., Shaula, A. L. *et al.*, Transport properties and thermal expansion of Ti-substituted $La_{1-x}Sr_xFeO_{3-\delta}$ ($x = 0.5$–0.7). *Solid State Sci.*, 2005, **7**, 355–365.
13. Diethelm, S., Van herle, J., Middleton, P. H. and Favrat, D., Oxygen permeation and stability of $La_{0.4}Ca_{0.6}Fe_{1-x}Co_xO_{3-\delta}$ ($x = 0, 0.25, 0.5$) membranes. *J. Power Sources*, 2003, **118**, 270–275.
14. Petric, A., Huang, P. and Tietz, F., Evaluation of La–Sr–Co–Fe–O perovskites for solid oxide fuel cells and gas separation membranes. *Solid State Ionics*, 2000, **135**, 719–725.
15. Stevenson, J. W., Armstrong, T. R., Carneim, R. D., Pederson, L. R. and Weber, W. J., Electrochemical properties of mixed conducting perovskites $La_{1-x}M_xCo_{1-y}Fe_yO_{3-\delta}$ (M = Sr, Ba, Ca). *J. Electrochem. Soc.*, 1996, **143**, 2722–2729.
16. Ritchie, J. T., Richardson, J. T. and Luss, D., Ceramic membrane reactor for synthesis gas production. *AiChE J.*, 2001, **47**, 2092–2101.
17. Atkinson, A. and Ramos, T. M. G. M., Chemically-induced stresses in ceramic oxygen ion-conducting membranes. *Solid State Ionics*, 2000, **129**, 259–269.
18. Yaremchenko, A. A., Patrakeev, M. V., Kharton, V. V., Marques, F. M. B., Leonidov, I. A. and Kozhevnikov, V. L., Oxygen ionic and electronic conductivity of $La_{0.3}Sr_{0.7}Fe(Al)O_{3-\delta}$ perovskites. *Solid State Sci.*, 2004, **6**, 357–366.
19. Fagg, D. P., Kharton, V. V., Frade, J. R. and Ferreira, A. A. L., Stability and mixed ionic-electronic conductivity of (Sr,La) (Ti,Fe)$O_{3-\delta}$ perovskites. *Solid State Ionics*, 2003, **156**, 45–57.
20. Kharton, V. V., Shaulo, A. L., Viskup, A. P., Avdeev, M., Yaramchenko, A. A., Patrakeev, M. V. *et al.*, Perovskite-like system (Sr,La)/(Fe,Ga)$O_{3-\delta}$: structure and ionic transport under oxidizing conditions. *Solid State Ionics*, 2002, **150**, 229–243.
21. Diethelm, S., Sfeir, J., Clemens, F., Van herle, J. and Favrat, D., Planar and tubular perovskite-type membranes reactors for the partial oxidation of methane to syngas. *J. Solid State Electrochem.*, 2004, **8**, 611–617.
22. Wang, H., Cong, Y. and Yang, W., Oxygen permeation study in a tubular $Ba_{0.5}Sr_{0.5}Co_{0.8}Fe_{0.2}O_{3-\delta}$ oxygen permeable membrane. *J. Membrane Sci.*, 2002, **210**, 259–271.
23. Trunec, M., Cihlar, J., Diethelm, S. and Van herle, J., Tubular $La_{0.7}Ca_{0.3}Fe_{0.85}Co_{0.15}O_{3-\delta}$ perovskite membranes. Part 1. Preparation and properties. *J. Am. Ceram. Soc.*, 2006, **89**, 949–954.
24. Bayraktar, D., Diethelm, S., Holtappels, P., Graule, T. and Van herle, H., Oxygen transport in $La_{0.5}Sr_{0.5}Fe_{1-y}Ti_yO_{3-\delta}$ ($y = 0, 0.2$) membranes. *J. Solid State Electrochem.*, 2006, **10**, 589–596.
25. Kharton, V. V., Yaremchenko, A. A., Patrakeev, M. V., Naumovich, E. N. and Marques, F. M. B., Thermal and chemical induced expansion of $La_{0.3}Sr_{0.7}(Fe,Ga)O_{3-\delta}$ ceramics. *J. Eur. Ceram. Soc.*, 2003, **23**, 1417–1426.